

## Real-Time Evaluation of Thin Film Drying Kinetics by an Advanced, Multi-Probe Optical Setup

Nusret S. Güldal,<sup>\*†</sup> Thaer Kassar,<sup>‡</sup> Marvin Berlinghof,<sup>‡</sup> Tayebah Ameri,<sup>†</sup> Andres Osvet,<sup>†</sup> Roberto Pacios,<sup>§</sup> Giovanni Li Destri,<sup>¶</sup> Tobias Unruh<sup>\*\*</sup> and Christoph J. Brabec<sup>†</sup>

<sup>†</sup>Materials for Energy Technology and Electronics, Friedrich-Alexander University Erlangen-Nürnberg, Martensstrasse 7, 91058, Erlangen, Germany

<sup>‡</sup>Chair for Crystallography and Structural Physics, Friedrich-Alexander University Erlangen-Nürnberg, Staudtstrasse 3, 91058, Erlangen, Germany

<sup>§</sup> IK4-IKERLAN, Paseo J.M. Arizmendiarieta 2, 20500, Arrasate-Mondragon, Spain and <sup>¶</sup> European Synchrotron Radiation Facility, 71 Avenue des Martyrs, 38000, Grenoble, France

### Supplementary Information

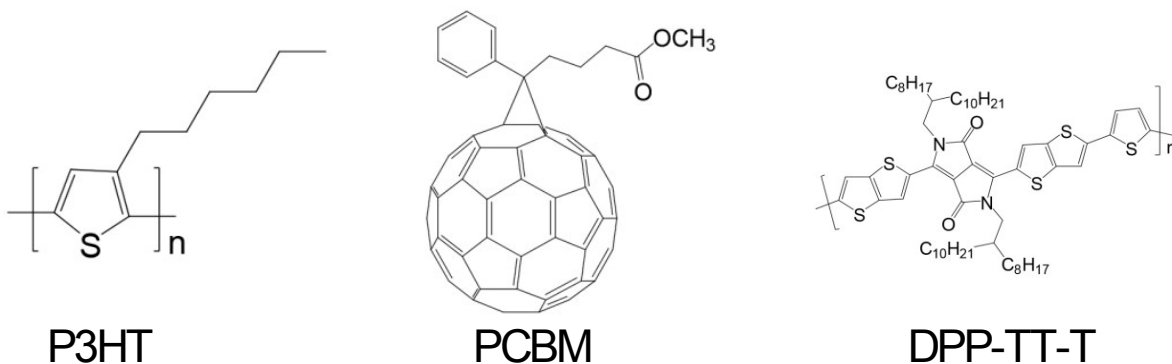


**Fig. S1** Chemical structures of P3HT, PCBM and DPP-TT-T.

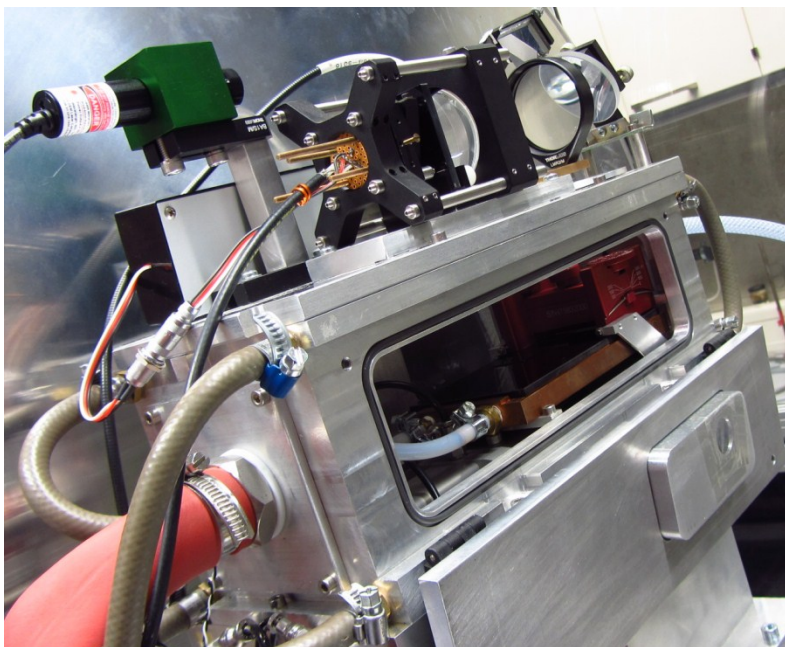


**Fig. S2** Picture of the *in situ* drying chamber used for the drying measurements, with the optical components installed on top.

### Section1. Light scattering discussion on pristine P3HT layer

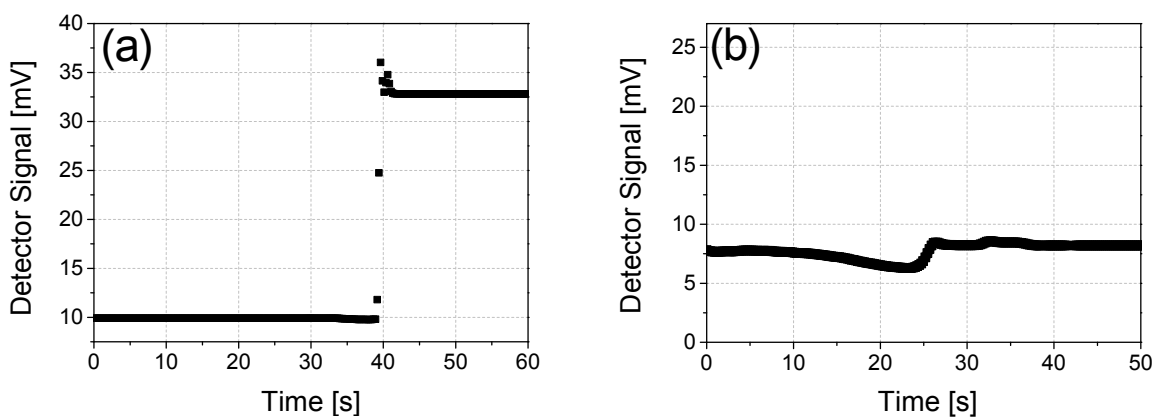
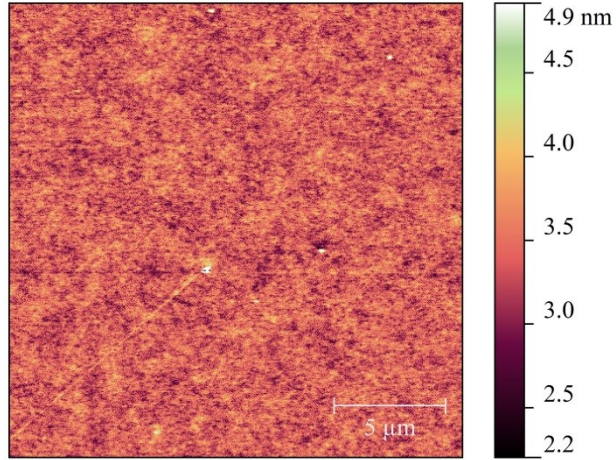


**Fig. S3** LS profiles of pristine P3HT (a) and DPP-TT-T (b). Measurements were conducted at the same conditions as blend drying measurements.

LS signal is generally seen right before the film dries completely. While DPP-TT-T barely shows any signal, pristine P3HT layer shows a significant signal, as seen above. This raises the question, for pristine layers like P3HT, if the signal originates from surface roughness. We have measured the AFM profile of the pristine P3HT layer and calculated that the root-mean-square roughness around 0.27 nm:



Theoretically, the ‘percentage’ of scattered light from an assumed 100 % total reflectance on a P3HT surface with around 1-nm roughness can be calculated as in the following<sup>1</sup>:

$$1 - \frac{R_S}{R_T} = \exp \left[ - \left( \frac{4\pi \cos \sigma R_{RMS}}{\lambda} \right)^2 \right]$$

where,  $R_S$  is specular reflectance,  $R_T$  is total reflectance,  $\sigma$  is incidence angle ( $34^\circ$ ),  $R_{RMS}$  is root-mean-square roughness (1 nm),  $\lambda$  is excitation wavelength (783 nm). Based on this calculation, on a P3HT layer with 1-nm roughness, there would be 0.02 % scattered light. Since the P3HT layer we have measured with LS has 0.27 nm roughness, the amount of scattered light will be even less. It is very unlikely that such small scattered signal from 0.27-nm rough surface would create mV-range signal when it is measured with a 783-nm laser, as seen in Fig. S3. Therefore, we conclude that the signal originates from coarse structures, which are in the order of our excitation wavelength.

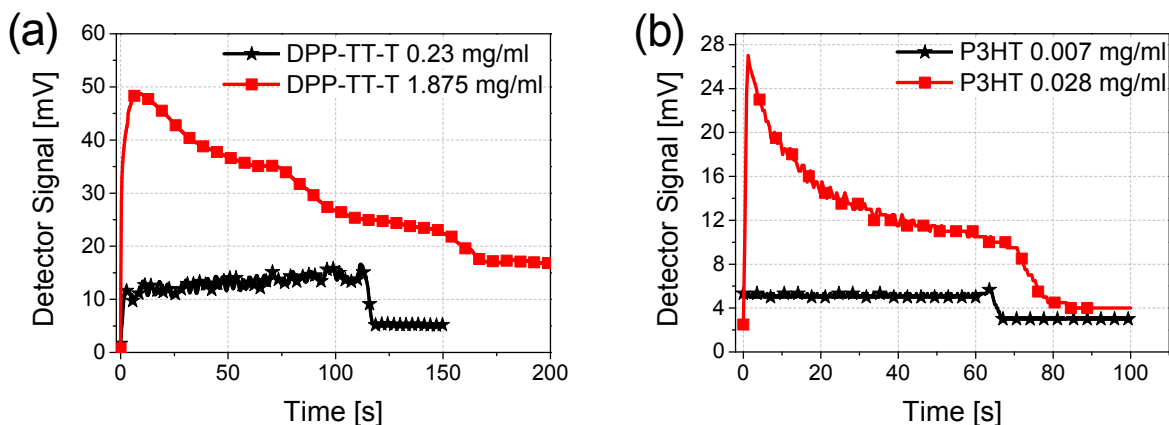


**Fig. S4** PL profiles of pristine DPP-TT-T (a) and P3HT (b). Measurements were conducted at room temperature with the given concentrations at each plot. With  $0.23 \text{ mg ml}^{-1}$  and  $0.007 \text{ mg ml}^{-1}$ , DPP-TT-T and P3HT, respectively, showed relatively constant PL behavior. Since samples are measured at room temperature, they had enough time for possible laser damage within the drying time. The signal stability for diluted samples indicates that instead of laser effects, PL patterns are dominated by the drying kinetics and thermodynamic effects.

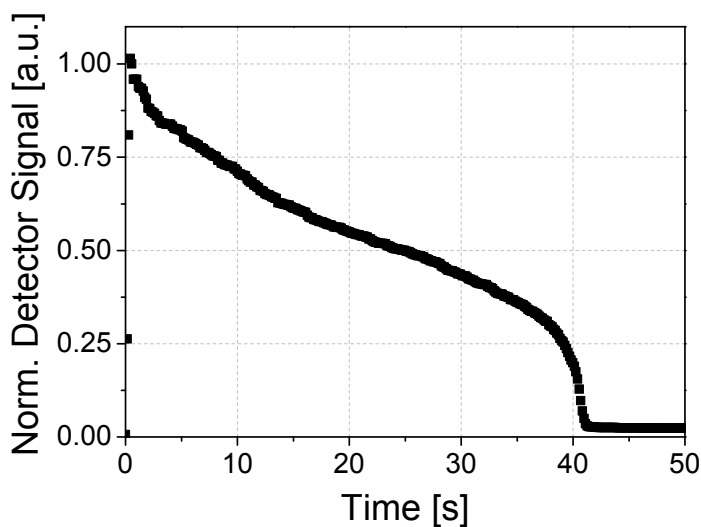


**Fig. S5** PL profile of pristine P3HT. The film was dried at the same conditions as the blend experiments ( $60^\circ\text{C}$ , He atmosphere, atmospheric pressure, on Si wafer). The starting solution was having the same concentration as the partial P3HT concentration of the blend solution ( $11.25 \text{ mg/mL}$ ). Here, close to the end of film drying, the concentration quenching is accompanied by aggregation quenching; hence the PL drop deviates from linear decay to exponential decay.

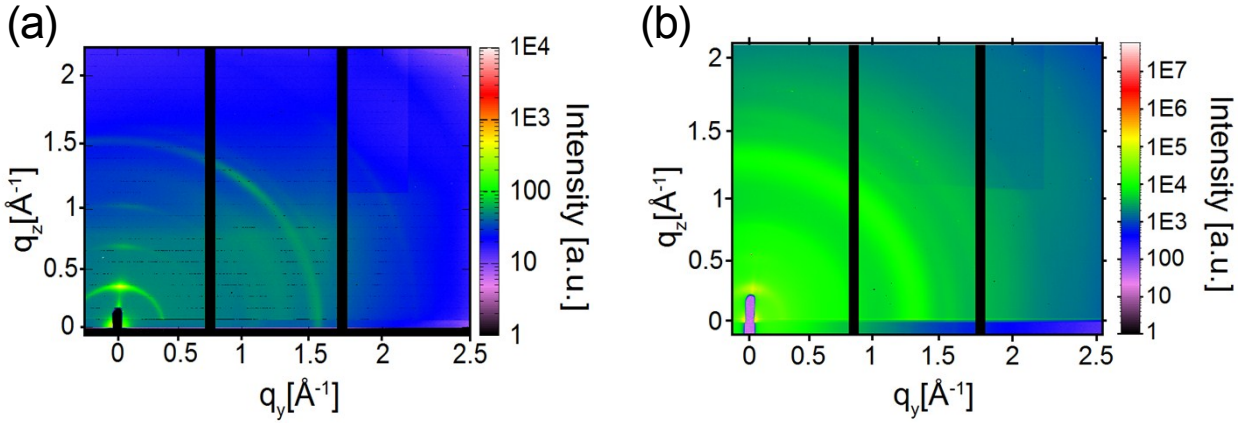


**Fig. S6** 2D GIXD pictures of fully dried P3HT:PCBM (a) and DPP-TT-T:PCBM (b).

The size  $D_{hkl}$  of a crystallite in a certain direction can be calculated using the Scherrer equation:

$$D_{hkl} = \frac{2\pi K}{\Delta q_{hkl}}$$

Here  $\Delta q_{hkl}$  is the FWHM of the corresponding peak (measured in  $q$ ). The Scherrer constant  $K$  is set to 0.9. The calculated size is systematically too small, because the peak is broadened by the non-zero size of the substrate.<sup>2</sup>

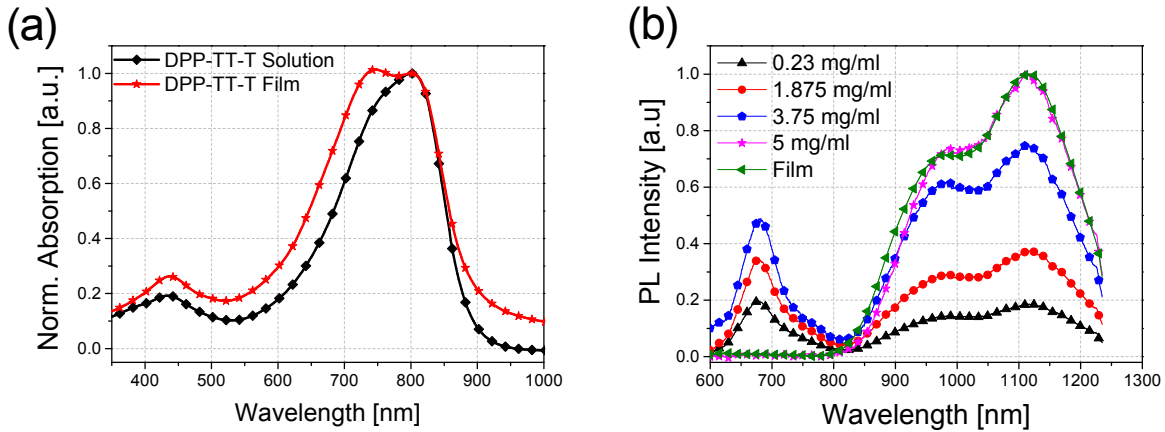


**Fig. S7** (a) UV-Vis absorption spectra of pristine DPP-TT-T in *o*-xylene:mesitylene mixture, measured from solution and film. (b) PL spectra of pristine DPP-TT-T solution in *o*-xylene:mesitylene at different concentrations and film.

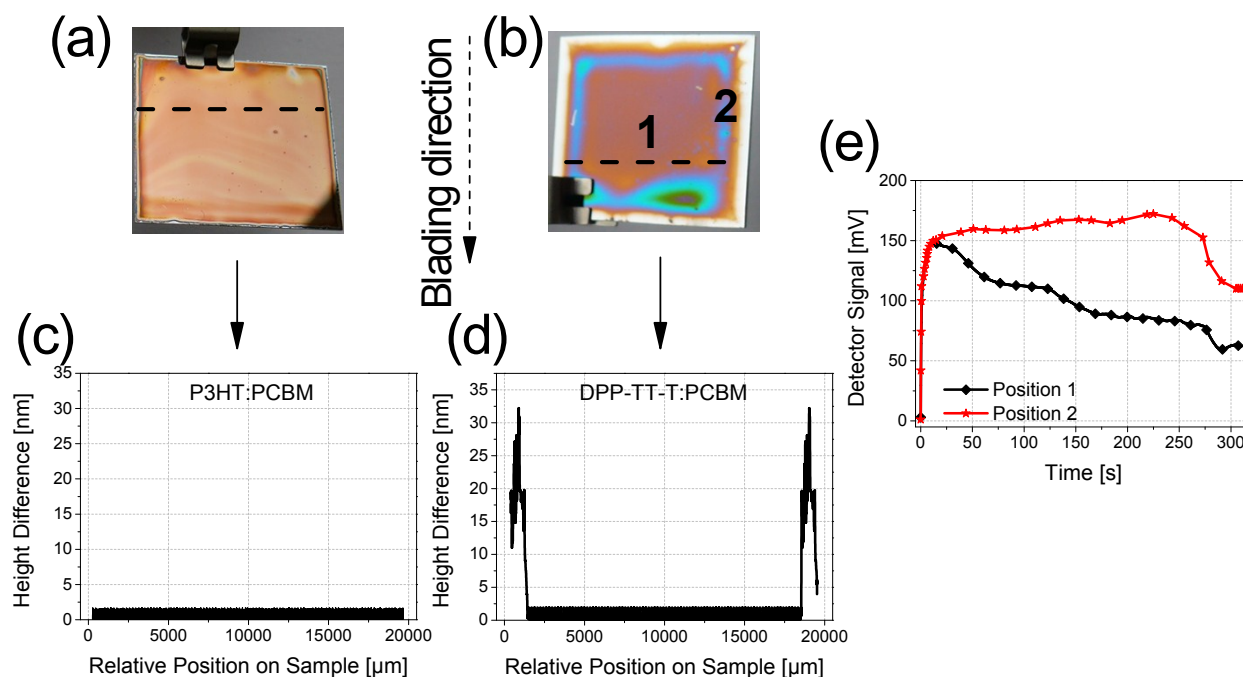


**Fig. S8** Sample film pictures of P3HT:PCBM (a) and DPP-TT-T:PCBM (b) on Si substrates after film deposition. The horizontal dashed lines indicate the lines at which height profiles are taken. The vertical dashed arrow shows the direction of blading. Corresponding height profiles are given in (c) and (d). *In situ* PL measurement comparison at different positions on DPP-TT-T:PCBM sample is given in (e). Positions are labeled accordingly in (b). As seen in (e), capillary flow towards the edges dominates the PL behavior until the 250<sup>th</sup> second at Position 2. This indicates that the capillary flow is present until the last moments of the drying process, constantly carrying DPP-TT-T from surroundings towards the edges constantly. However, at Position 1, where *in situ* drying measurements were conducted, capillary flow induces the initial decrease by removing some of the polymer, and afterward, concentration quenching dominates the PL behavior.

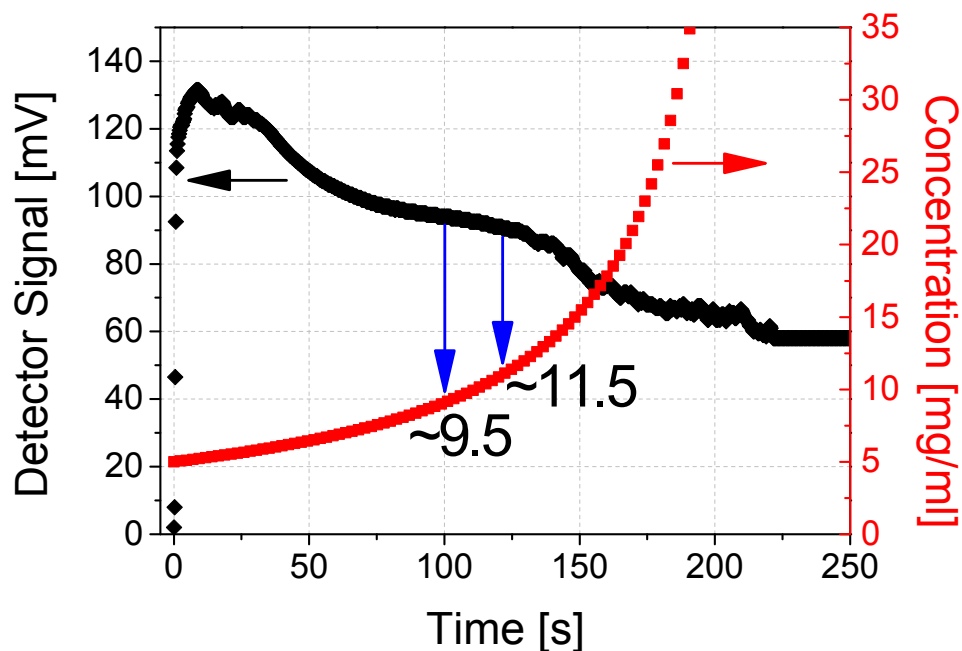


**Fig. S9** *In situ* PL measurement of pristine DPP-TT-T in o-xylene with concentration of 5 mg mL<sup>-1</sup>. Vertical arrows indicate the concentration values to the corresponding PL data. Horizontal arrows show the corresponding y-axis for each plot. Concentration profile was calculated from the drying curve, which is not shown. The solubility measurements for pristine DPP-TT-T in o-xylene at room temperature were measured as 9.5 mg mL<sup>-1</sup>, which corresponds to the same PL region observed in blend measurements.

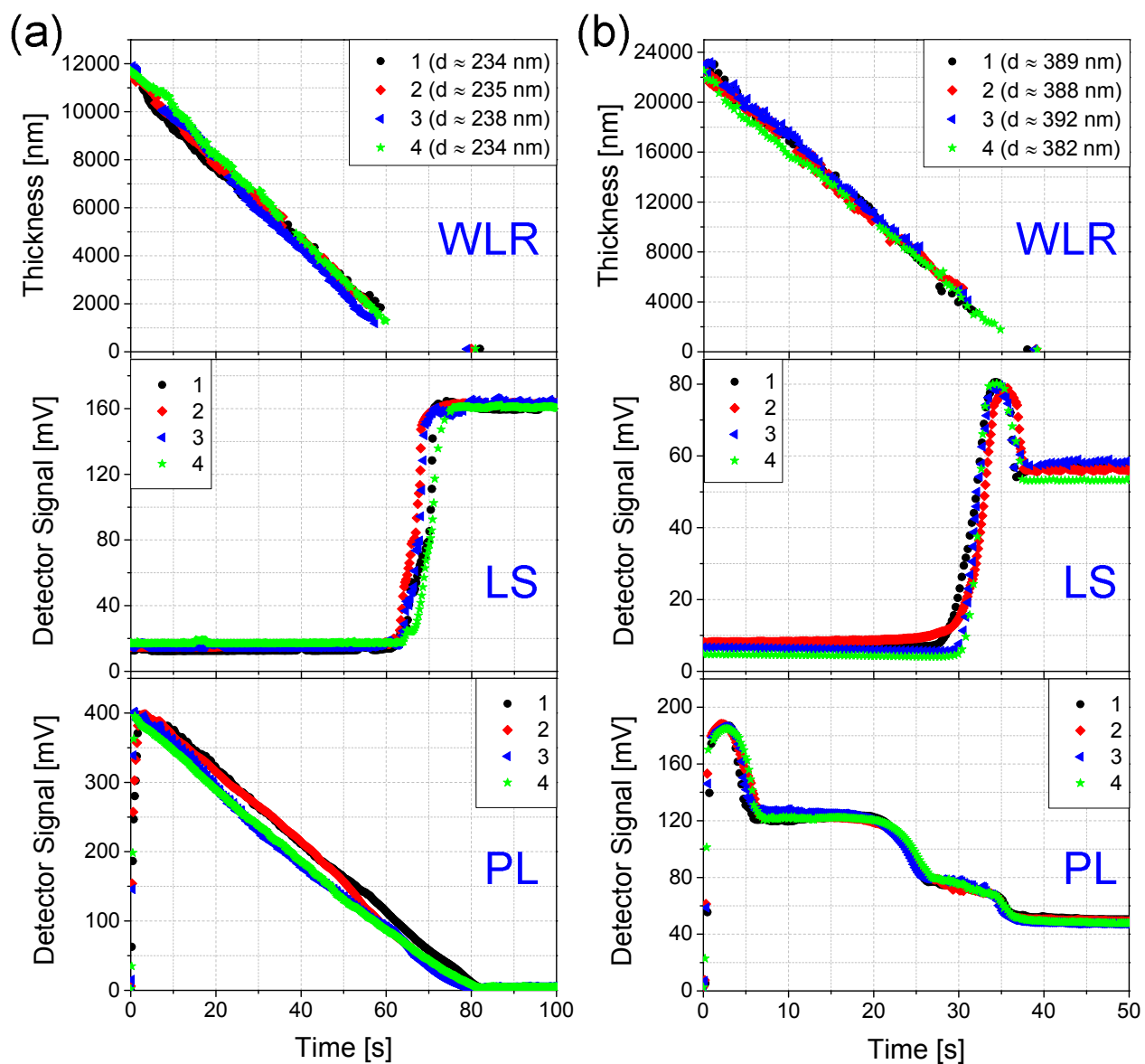
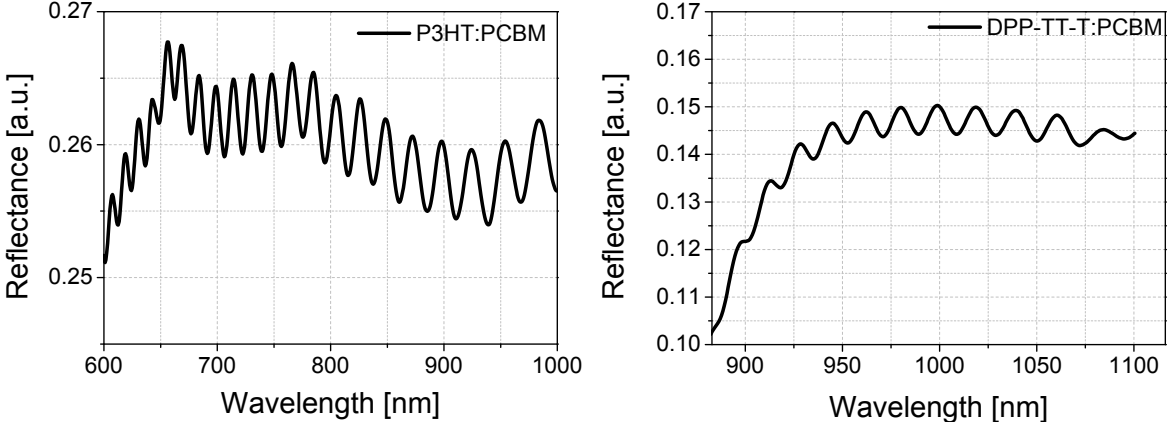


**Fig. S10** Statistical measurements of (a) P3HT:PCBM and (b) DPP-TT-T:PCBM drying. Each blend was measured 4 times under exact same drying conditions. WLR plots are the results measured together with PL. The legend for each WLR plot includes thickness values of dried layers for comparison. Measurements labeled as ‘1’ (black circle) are the measurements conducted for the main article text. Measurements labeled as ‘2’, ‘3’ and ‘4’ were conducted much later than ‘1’, thus the synchrotron studies were not possible. Nevertheless, WLR, LS and PL results and end thickness values for each blend confirm very strongly that the *in situ* drying chamber can be operated under exact same drying conditions any time.



## Section 2. Summary on calculation of thickness from white-light reflectometry

Thickness values from reflectance spectrum for each sample were calculated based on the interference theory. Example spectra for P3HT:PCBM and DPP-TT-T:PCBM on Si wafer with natural SiO<sub>2</sub> layer are presented in the following:



Theoretically as the thickness reduces, fringes would be also observed at higher energy regions. Thickness calculations in these regions (UV-600 nm for P3HT:PCBM and UV-900 nm for DPP-TT-T:PCBM) should be conducted very carefully since these regions contain several different information (Si wafer reflectance, Si wafer absorption, coated film absorption, reflection of the layer surface, interference fringes...). Firstly, some of these effects damp the interference fringes heavily, and secondly, absorption information of the coated film is not reliable for any sort of comparison. Therefore, the wavelength range (IR) for thickness calculations was selected in a way that these effects are minimized. In the IR region, we only have Si wafer absorption, which reduces the signal, but not disturbing interference fringes.

For a reflection of a film on a substrate with higher refractive index, superposition of two reflected waves can have two distinct cases with respect to the path difference:

$$\Delta_{const.} \rightarrow 2dn = m\lambda$$

$$\Delta_{destr.} \rightarrow 2dn = \left(m + \frac{1}{2}\right)\lambda$$

where  $\lambda$  is the wavelength,  $d$  is film thickness, and  $n$  is refractive index. Based on these equations, film thickness for a layer which has different refractive indices at different wavelengths can be calculated from two adjacent maxima (or minima) as in the following:

$$d = \frac{\lambda_1 \lambda_2}{2(\lambda_1 n_2 - \lambda_2 n_1)}$$

This calculation is very accurate if the refractive indices are handled correctly. For this manuscript, we calculated the dielectric functions of P3HT:PCBM and DPP-TT-T:PCBM solutions at different concentrations via Effective Medium Approximation (Bruggeman). Dielectric functions of the solvents and dried layers of P3HT:PCBM and DPP-TT-T:PCBM were measured with spectroscopic ellipsometry (Woollam M-2000). Effective Medium Approximation was then conducted in commercially available software WVASE™.

It should be noted that, close to the final drying (approx. starting from 60<sup>th</sup> second for P3HT:PCBM sample and from 30<sup>th</sup> second for DPP-TT-T:PCBM), thickness values cannot be calculated due to interference losses. These losses occur due to the strong changes in the dielectric functions of these blends close to the drying, especially due to their anisotropic character. These regions can be resolved and modelled by ellipsometry properly, when it is needed. Although we cannot resolve these drying regions with reflectometry measurements, the time point for the end of drying can be recognized as the time point at which the spectrum stops changing. Lastly, the dried layer thicknesses were measured with a profilometer.

- 1 J. E. Harvey, S. Schröder, N. Choi, and A. Duppore, *Opt. Eng.*, 2012, **51**, 1, 013402.
- 2 D.-M. Smilgies, *J. Appl. Crystallogr.*, 2009, **42**, 6, 1030–1034.